CLOUDINESS VARIABILITY OVER THE SOUTHWESTERN ATLANTIC REGION

Moira Luz Clara[1,2,3], Reinaldo A. Maenza[1], Robert Frouin[4], Vivian Lutz[1,2], Ana I. Dogliotti[3,5]
mluzclara@inidep.edu.ar

[1]Instituto Nacional de Investigación y Desarrollo Pesquero (INIDEP)
[2]Consejo Nacional de Investigaciones Científicas y Técnicas (IIMyC - CONICET)
[3]Instituto Franco-Argentino para el Estudio del Clima y sus Impactos (IRL IFAECI/CNRS-IRD-CONICET-UBA)
[4]Climate, Atmospheric Science, and Physical Oceanography Division, Scripps Institution of Oceanography, University of California, San Diego, La Jolla, CA, USA
[5]Instituto de Astronomía y Física del Espacio (IAFE), CONICET-Universidad de Buenos Aires.

Key words: co-variability, marine primary production, climate indices.

1) INTRODUCTION

Marine primary productivity strongly depends on light availability to assimilate and fix inorganic carbon into organic matter. Hence, the analysis of cloudiness variability over the ocean, such as the "in-cloud optical thickness" (a measure of the attenuation of the sunlight caused by the scattering and reflection from cloud droplets) are useful to understand primary production variability over a region.

2) DATA AND METHODOLOGY

The input data are monthly fields of in-cloud optical thickness of all clouds ('tottau', hereafter) from the MERRA-2 reanalysis (GMAO, 2015). The analyzed domain extends from 65°S up to 30°S and 70°W to 45°W for the period 1998/01 – 2019/12. The horizontal resolution of the MERRA-2 data is 0.5° latitude by 0.625° longitude.

Firstly, to determine subregions of spatially homogeneous cloudiness variability the rotated S-mode Principal Component Analysis (Richman, 1986; RSPCA, hereafter) was applied. The Varimax criterion (Kaiser, 1958) was selected for rotation, ensuring the orthogonality of modes and the correlation matrix was used as similarity matrix for the input to RSPCA. We usually refer to individually rotated principal components as modes, their spatial patterns as loading maps, and their time series as scores. Since the output of RSPCA can be a statistical artifact of the methodology (Richman 1986), a comparison of loading maps and the corresponding one-point correlation maps (autocorrelation maps, hereafter) was performed to ensure the reliability of the variability modes. The seasonal cycle was removed and the continental area was masked in the analysis.

Finally, the linkage between the climate forcings and scores was studied by applying the Cross Wavelet Transform (XWT) to expose the high common power and relative phase in time-frequency space between the scores and time series related to climatic indices such as the observational Southern Annular Mode index (SAM; Marshall 2003); Tropical South Atlantic Index (TSA; Enfield et al., 1999), Southern Oscillation Index (SOI), El Niño 1.2/3/3.4/4 (Takahashi et al., 2011) and the Ocean El Niño index (ONI) provided by the NOAA (all of them retrieved from http://www.esrl.noaa.gov/); and the Indian Ocean Dipole (IOD) provided by the Japan Agency for Marine-Earth Science and Technology (retrieved from http://www.jamstec.go.jp); among others.

3) RESULTS AND DISCUSSION

The rotated loading maps and the corresponding autocorrelation maps are displayed in Figure 1, ordered from the highest to the lowest in explaining variances. Three principal components were retained and rotated following the Kaiser criterion, explaining about 30.1%, 19.45%, and 17.35% of total variances, respectively.

The similarities between loadings and autocorrelation maps are discernible, ensuring that the variability modes describe real variability modes contained in the dataset. A main action center is denoted on every loading map with loading-values over 0.9, so every score (figures not shown) describes the variability for a particular region of the Southwestern Atlantic. The action centers are located close to 47.5°S - 53.125°W, 57°S - 57.5°W, and 37.5°S - 50.625°W, which oceanographically correspond approximately to the east of the Shelf-break Front, the Drake Passage, and the Malvinas-Brazil Confluence Zone, respectively.

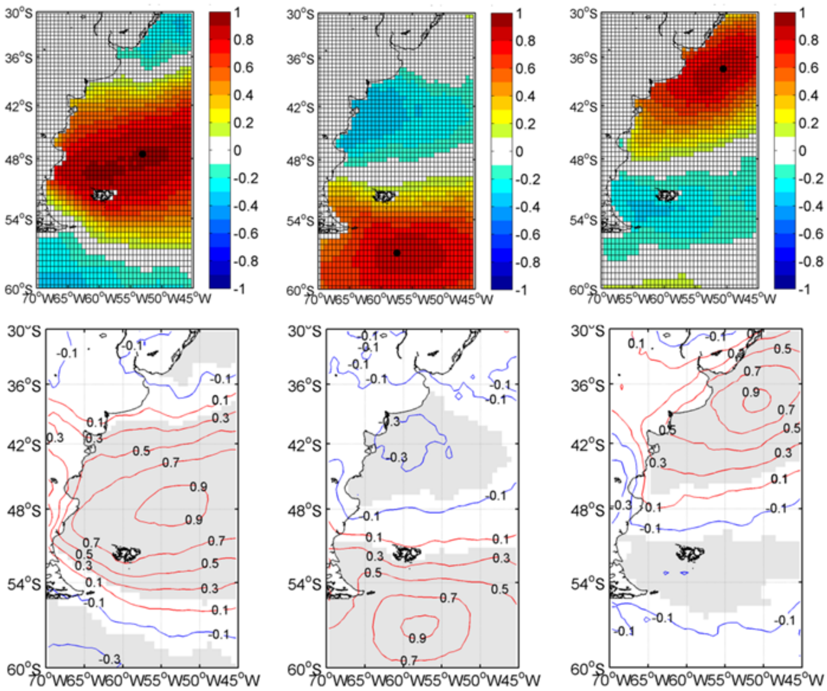

Figure 1. Rotated loading maps for the three retained modes (top panels) and the corresponding one-point correlation maps for the points with highest loadings for the modes displayed in the top panel. Figures are ordered from the highest to the lowest in explaining variances. Gray shaded areas denote statistically significant Pearson correlation coefficient at 95% confidence level.

The stationary and non-stationary co-variability between rotated scores and climate indices is displayed in Figure 2 by means of XWT. Only XWT with statistically significant quasi-oscillations among the time series is shown. Anti-phase quasi-cycles with the oceanic component of El Niño variability mode, and in-phase quasi-oscillations with SAM are observed, both in periodicities within the bandwidth of 2-3 year (low-frequency variability). The SAM influence is stronger at middle and high latitudes (rotated modes 1 and 2) and sporadic for the three regions (the links are observed during short sub-periods). Even though the sea surface temperature variability over the Pacific Tropical Ocean influences cloudiness over the entire studied area, it does it especially in the extratropical region (rotated mode 3) during a longer period.

These preliminary results show that there are regions of marked variability in cloudiness over the Southwestern Atlantic ocean, though even the first RSPCAs do not explain a high percentage of variability, which denote the heterogeneity of conditions in the region. The co-variability between rotated scores and climate indices showed patterns of similarities during certain periods. Further analyses will be conducted to interpret the cloudiness variability, its possible relation to climate change, and its impact on marine primary production.

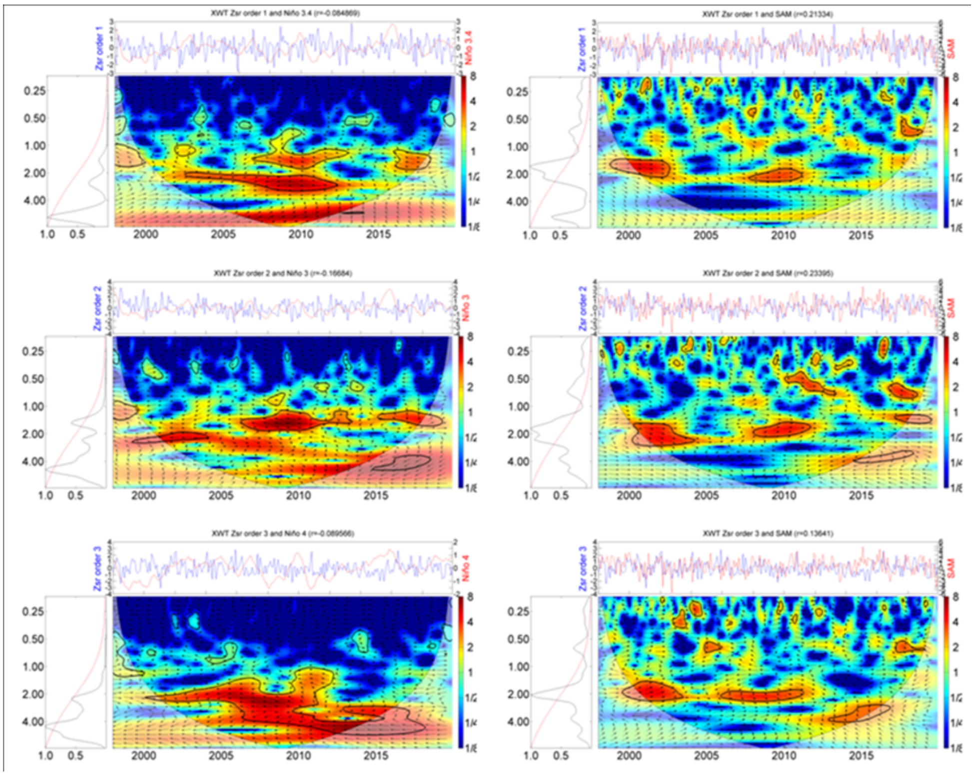

Figure 2: Cross wavelet transform of the standardized rotated loading order 1 (top), order 2 (middle), and order 3 (bottom) and climate indices El Niño (left) and SAM (right) using Morlet wavelet. Charts on top: standardized rotated loading (blue line) and climate index time series (red line). Charts on the left side: global wavelet spectrum (black solid line) and confidence interval (red solid line). The left axis is the Fourier period (year). Charts on the right side: The bottom axis is time (year). The relative phase relationship is shown as arrows (with in-phase pointing right and anti-phase pointing left). Solid thick contour encloses 95% of confidence level. The cone of influence where edge effects become important is shown as a lighter shade. The color bar represents the normalized power of the cross wavelet.

REFERENCES

Enfield, D.B., Mestas, A.M., Mayer, D.A., y Cid-Serrano, L., 1999: How ubiquitous is the dipole relationship in tropical Atlantic sea surface temperatures? J. Geophys. Res. 104: 7841–7848.

GMAO (Global Modeling and Assimilation Office), 2015: MERRA-2 3D IAU State, Meteorology Instantaneous 3-hourly (p-coord, 0.625x0.5L42), version 5.12.4, Greenbelt, MD, USA: Goddard Space Flight Center Distributed Active Archive Center (GSFC DAAC).

Kaiser, H.F., 1958: The Varimax criterion for analytic rotation in factor analysis. Psychometrika 23(3): 187–200.

Marshall, G.J., 2003: Trends in the Southern Annular Mode from observations and reanalyses. J. Clim. 16: 4134–4143.

Richman, M.B., 1986: Rotation of principal components. J. Climatol. 6: 293–335.

Takahashi, K., Montecinos, A., Goubanova, K., y Dewitte, B., 2011: ENSO regimes: reinterpreting the canonical and Modoki El Niño. Geophys. Res. Lett. 38: L10704.